NASA TECHNICAL NOTE

NASA TN D-3281

AN ANALYSIS OF AEROELASTIC DIVERGENCE IN UNGUIDED LAUNCH VEHICLES

by Vernon L. Alley, Jr., and A. Harper Gerringer

Langley Research Center
Langley Station, Hampton, Va.

NATIONAL AERONAUTICS AND SPACE ADMINISTRATION • WASHINGTON, D. C. • MARCH 1966

NASA TN D-3281

AN ANALYSIS OF AEROELASTIC DIVERGENCE IN UNGUIDED LAUNCH VEHICLES

By Vernon L. Alley, Jr., and A. Harper Gerringer

Langley Research Center
Langley Station, Hampton, Va.

NATIONAL AERONAUTICS AND SPACE ADMINISTRATION

For sale by the Clearinghouse for Federal Scientific and Technical Information
Springfield, Virginia 22151 – Price $2.00

AN ANALYSIS OF AEROELASTIC DIVERGENCE IN UNGUIDED LAUNCH VEHICLES

By Vernon L. Alley, Jr., and A. Harper Gerringer
Langley Research Center

SUMMARY

A discrete-system matrix method is developed for analyzing the aeroelastic divergence behavior of slender-body unguided launch vehicles. The solution is of the form of an eigenvalue problem that yields a divergence dynamic pressure at which divergent flight behavior will occur. A means for computing a generalized static margin that includes aeroelastic effects for the flexible vehicle is also proposed. Data necessary to accomplish an analysis are illustrated, along with example outputs. A parametric study is included to show the sensitivity of the divergence dynamic pressure and generalized static margin to variations in fin-lift characteristics. Stability criteria relating to the divergence dynamic pressure and the generalized static margin are suggested for both rigid or flexible vehicles, including those of extreme slenderness. It is believed that adherence to the suggested criteria will preclude destructive divergent behavior as well as minimize weight penalties due to aeroelastic load magnifications. The aeroelastic divergence study is shown to be necessary in establishing a compatibility between the aerodynamic and structural design.

INTRODUCTION

The evaluation of aeroelastic divergence characteristics is an important function in qualifying the aerodynamic and structural compatibility of a new launch vehicle configuration. Aeroelastic divergence theory specifically oriented to slender bodies is particularly necessary by virtue of the high performance of present-day space launch vehicles. The divergence problem is essentially restricted to the ascent phase of flight where the multistages are intact and the atmosphere has an appreciable effect. A similar problem is sometimes encountered in models mounted on flexible sting supports in wind tunnels.

Although there is a substantial body of literature on aircraft wing divergence (see ref. 1), limited published work is available on divergence for direct application to launch vehicles. Arbic, White, and Gillespie recognized the problem in the early 1950's and in reference 2 presented approximate methods for estimating the effects of aeroelastic

bending on launch vehicles. The Australians encountered the problem in 1959 in the development of a three-stage launch vehicle and subsequently published an approximate theory, along with comparative experimental and theoretical data, in reference 3.

Both references 2 and 3 approach the aeroelastic behavior of the system as a nonhomogeneous load problem. Vehicle loads and deflections are computed in terms of an assumed initial trim, or misalinement, and deflection magnifications due to elastic contributions are determined. This approach does not directly yield critical stability roots but can be used to imply impending instability as the elastic deflections become increasingly larger or as the stabilizing moment becomes increasingly smaller as larger dynamic pressures are used in trial solutions. It is also true of reference 3 and for some of the methods of reference 2 that the flexibility contributions are unnecessarily restricted to the upper stages of the vehicle. This restriction is inherent to the solutions by virtue of the assumption that the predominantly flexible portion of the vehicle is considered referenced to an assumed rigid portion such as the first stage.

The purpose of this paper is to present a systematic mathematical approach to the problem of aeroelastic divergence as applied to launch vehicles. The method presented is a true stability analysis in the sense that it determines the possible states of equilibrium that would occur by virtue of only the critical combinations of system variables and does not involve any independent external stimuli. There are no nonhomogeneous loads in the equations of motion. In addition, the method imposes no limitations, such as were employed in reference 3, on the treatment of flexibility. Mathematically, the equations of equilibrium constitute a typical eigenvalue, eigenfunction problem. In addition, consideration is given to defining and computing a parameter for a flexible vehicle, called the generalized static margin, that is a measure of stability analogous to the rigid-body static margin. Numerical results consisting of divergence dynamic pressures and generalized static margins for an actual research launch vehicle are also included.

SYMBOLS

The units of measurement originally used in this analysis were in the U.S. Customary System. To increase the usefulness of the report, however, alternate values are given in the International System, which is abbreviated internationally as SI. Details of this system and conversion factors are presented in reference 4. SI units herein are in parenthesis.

A	square matrix of equation (14), radians/pound force (radians/newton)
c_u	coordinate to the uth joint measured from the x origin, inches (meters)
$C_{N_\alpha}S_0$	product of normal-force-coefficient slope and relative panel area of zero station, inch^2/radian (meter^2/radian)

$C_{N_\alpha}S_{div}$	product of normal-force-coefficient slope and area of zero station compatible with a $q/q_{div} = 1$, inch^2/radian (meter^2/radian)
$C_{N_\alpha}S_{mar}$	product of normal-force-coefficient slope and marginal area above divergence value of $C_{N_\alpha}S_{div}$, inch^2/radian (meter^2/radian)
$\overline{C_{N_\alpha}S}$	product of total normal-force-coefficient slope and total reference area, inch^2/radian (meter^2/radian)
$C_{N_\alpha}S_r$	product of normal-force-coefficient slope and panel area of the rth station, inch^2/radian (meter^2/radian)
D_{max}	maximum body diameter of staging, inches (meters)
E	flexural modulus of elasticity, pounds force/inch^2 (newtons/meter^2)
C_{N_α}	normal-force-coefficient slope, $\partial C_N/\partial\alpha$
F_r	total transverse force acting at rth station, pounds force (newtons)
I	moment of inertia of cross-sectional area of structural members, inch^4 (meter^4)
L	overall length of vehicle, inches (meters)
M	total mass of vehicle, pound force-second^2/inch (newton-second^2/meter)
m_r	mass of rth discrete element, pound force-second^2/inch (newton-second^2/meter)
p	total number of discrete elements comprising analogous system
P_r	total axial force acting on rth station parallel to x-axis, pounds force (newtons)
q	dynamic pressure of airstream for condition under study, pounds force/inch^2 (newtons/meter^2)
q_{div}	dynamic pressure at which aeroelastic divergence would occur, pounds force/inch^2 (newtons/meter^2)
R	radius of curvature of flight path at $x = 0$, inches (meters)
r	subscript defining discrete elements
T	thrust, pounds force (newtons)

u,v	velocity components of origin of axes parallel to x- and y-axes, respectively, inches/second (meters/second)
W	weight per unit length, pounds force/inch (newtons/meter)
x	independent coordinate along vehicle body and tangent to elastic axis at $x = 0$, inches (meters)
x_{cg}	distance from x-origin to center of gravity, inches (meters)
x_{cp}	distance from x-origin to center of pressure, inches (meters)
x_{gsm}	generalized static margin, inches (meters)
x_{sm}	static margin, $x_{cg} - x_{cp}$, inches (meters)
$x_{sm,rig}$	static margin of rigid vehicle, inches (meters)
y	elastic deflection of vehicle relative to tangent to elastic axis at $x = 0$, inches (meters)
α	angle of attack, radians
α_r	angle of attack at rth station, radians
$\dot{\gamma}$	angular velocity about an axis normal to x,y axes, radians/second
κ_u	local rotation at c_u due to joint flexibility, radians/inch-pound force (radians/meter-newton)
λ	eigenvalue, radians/pound force (radians/newton)
$\rho_{r,n}$	total slope influence coefficient; slope at $x = x_r$ due to a unit load at $x = x_n$ when cantilevered at $x = 0$, radians/pound force (radians/newton)
$\{\ \}, [\ ], [\ ], [\ ], [1]$	column, diagonal, square, row, and unit matrices, respectively

Subscripts:

n,r	discrete elements
0	zero-station element

THEORY

The assumptions underlying the analysis and derivations of the equations of equilibrium and the expression for the generalized static margin are set forth in the following section.

Assumptions

The major assumptions incorporated in the development of the equilibrium equations are listed as follows.

Beam theory.- It is assumed that elastic deformations of the vehicle body are described by elementary bending theory of beams. The usual assumptions of small deflections are utilized. All effects due to axial loads are considered to be negligible.

Plane analysis.- The problem is restricted to the consideration of divergent behavior in a single plane of motion. Only linear homogeneous loads are considered and accelerations due to gravity are thus precluded.

Nonspinning vehicle.- The vehicle is considered as nonspinning. In applications to vehicles of low spin rates useful approximate results may be obtained for the spinning vehicle.

Discrete representation.- A discrete mass representation of the actual structure is used. Local aerodynamic panels are also assumed to be associated with each discrete mass.

Panel aerodynamics.- The solution requires linear aerodynamic normal-force derivatives for the various lift panels of the discrete representation of the vehicle. The normal forces produced by each aerodynamic panel are assumed proportional to the products of their local angles of attack and specified normal-force derivatives. Also, the assumption of small angles of attack is made. Aerodynamic force coupling between panels (downwash) may be accounted for in the rigid-body portion of the displacement (v/u) by utilizing an appropriate aerodynamic lift derivative distribution. However, coupling between panels due to aerodynamic changes associated with the elastic deformation of the system cannot be accounted for within the framework of the formulation. Furthermore, angles of attack resulting from cross flow induced by the angular velocity of the vehicle are ignored. Drag influences are also neglected.

Steady-state analysis.- The formulation treats the structure as being frozen in a nonoscillatory steady state of dynamic equilibrium for a particular set of conditions associated with a given time in flight. The centripetal acceleration at the origin of the coordinate system due to curvilinear flight is considered the only significant inertia effect and is considered to act normal to the vehicle longitudinal body axis and to be

invariant over the vehicle span. This procedure is justified for small angles of attack, small elastic displacements, and when the length of the vehicle is small in comparison with the radius of curvature of the flight path.

Equations of Equilibrium

In sketch A a discrete element of a deflected beam is shown subjected to aerodynamic and inertia forces compatible with the foregoing assumptions. The coordinates x and y to the element are for body-fixed axes. The origin of x and y is taken near the left end of the beam at the center of the first discrete element with the x axis taken tangent to the elastic axis. The quantities u and v are the velocity components of the origin parallel to the x- and y-axes, respectively.

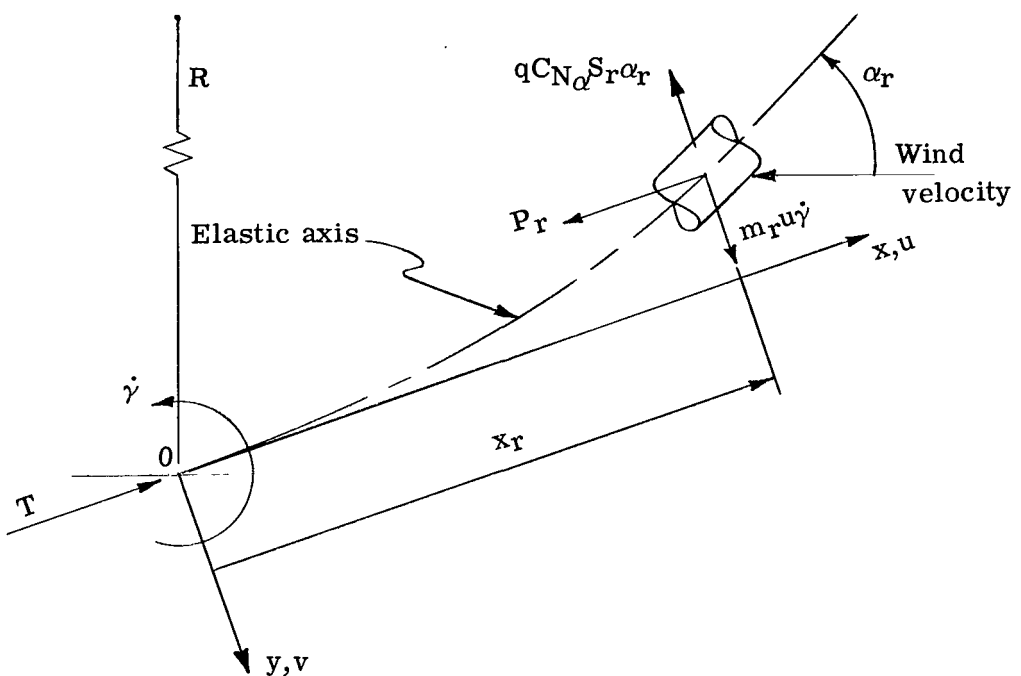

Sketch A

In keeping with the aerodynamic assumptions, the normal force generated on the rth discrete element of the beam can be expressed as $qC_{N_\alpha}S_r\alpha_r$. Also, in view of the assumptions of planar motion and steady-state conditions, the transverse inertia loading of the rth element is simply $m_r u\dot{\gamma}$. This quantity is equivalent to $m_r R\dot{\gamma}^2$, which is more recognizable as the centrifugal force. Thus, the total transverse force generated on the rth element is given by

$$F_r = m_r u\dot{\gamma} - qC_{N_\alpha}S_r\alpha_r \tag{1}$$

where F_r is assumed positive in the direction of positive y. The local angle of attack α_r at the rth element can be adequately defined, for small angles of attack, as

$$\alpha_r \approx \frac{v}{u} - \left(\frac{dy}{dx}\right)_r \tag{2}$$

If column bending action is ignored, then the deflection-load relationships can conveniently be expressed in terms of influence coefficients. Such coefficients can be determined by a number of analytical processes or by actual measurements. Some details relative to computing appropriate slope influence coefficients are given in a subsequent section. Let $\rho_{r,n}$ denote the slope at station r due to a unit transverse force at station n for a cantilever beam fixed at $x = 0$. Then the slope at $x = x_r$ due to all of the loads acting on a total of p discrete elements can be described as

$$\left(\frac{dy}{dx}\right)_r = \sum_{n=1}^{p-1} \rho_{r,n} F_n \tag{3}$$

It should be observed that by virtue of the assumption of cantilever beam influence coefficients, $\rho_{0,n} = 0$, and consequently the summation need only be extended from 1 to p - 1. Furthermore, it should be noted that if the first element on the left is designated as the zeroth element of a total of p stations, then the last element on the right is the p - 1 station.

Substituting equation (3) into equation (2) and the resulting expression into equation (1) yields the following equation:

$$F_r = m_r u\dot{\gamma} - qC_{N_\alpha} S_r \left(\frac{v}{u} - \sum_{n=1}^{p-1} \rho_{r,n} F_n \right) \tag{4}$$

Equation (4) can be conveniently written in matrix form for all values of r from 1 to p - 1:

$$\{F_r\} = u\dot{\gamma}\{m_r\} - q\frac{v}{u}\left[C_{N_\alpha} S_r\right]\{1\} + q\left[C_{N_\alpha} S_r\right]\left[\rho_{r,n}\right]\{F_n\} \tag{5}$$

where r,n = 1, 2, 3, . . ., p - 1. For translational and rotational equilibrium to exist, the following two relationships must be satisfied:

$$\left[1\right]\{F_r\} + F_0 = 0 \tag{6}$$

$$\left[x_r\right]\left\{F_r\right\} = 0 \tag{7}$$

where $r = 1, 2, 3, \ldots, (p - 1)$ and the moment contributions due to the column forces P_r have been neglected. This omission is acceptable by virtue of the assumption of small displacements as long as the thrust T remains well below the critical buckling thrust for the column under free-free boundary conditions.

It is important to note at this point that satisfying equations (6) and (7) will effectively remove the artificial cantilever boundary conditions used in obtaining the influence coefficients $\rho_{r,n}$. Also, it is now expedient to introduce the following terms:

$$\left.\begin{aligned} M &= \left[1\right]\left\{m_r\right\} + m_0 \\ Mx_{cg} &= \left[x_r\right]\left\{m_r\right\} \\ \overline{C_{N_\alpha}S} &= \left[1\right]\left[C_{N_\alpha}S_r\right]\left\{1\right\} + C_{N_\alpha}S_0 \\ x_{cp}\overline{C_{N_\alpha}S} &= \left[x_r\right]\left[C_{N_\alpha}S_r\right]\left\{1\right\} \end{aligned}\right\} \quad (r = 1, 2, 3, \ldots, (p - 1)) \tag{8}$$

Furthermore, note from equations (1) and (2) that when $r = 0$,

$$F_0 = m_0 u\dot{\gamma} - qC_{N_\alpha}S_0 \frac{v}{u} \tag{9}$$

Utilizing the above notations and operating upon equation (5) in accordance with equations (6) and (7) yields two equations in terms of the unknowns $u\dot{\gamma}$, v/u, and the column matrix F_n. Thus,

$$Mu\dot{\gamma} - q\frac{v}{u}\overline{C_{N_\alpha}S} = -q\left[1\right]\left[C_{N_\alpha}S_r\right]\left[\rho_{r,n}\right]\left\{F_n\right\} \tag{10}$$

$$Mu\dot{\gamma} - q\frac{v}{u}\overline{C_{N_\alpha}S}\frac{x_{cp}}{x_{cg}} = -q\left[\frac{x_r}{x_{cg}}\right]\left[C_{N_\alpha}S_r\right]\left[\rho_{r,n}\right]\left\{F_n\right\} \tag{11}$$

Solving equations (10) and (11) simultaneously for $u\dot{\gamma}$ and v/u gives

$$u\dot{\gamma} = \frac{q\left[\frac{x_{cp}}{x_{cg}} - \frac{x_r}{x_{cg}}\right]\left[C_{N_\alpha}S_r\right]\left[\rho_{r,n}\right]\left\{F_n\right\}}{M\left(1 - \frac{x_{cp}}{x_{cg}}\right)} \tag{12}$$

$$\frac{v}{u} = \frac{\left[1 - \frac{x_r}{x_{cg}}\right]\left[C_{N_\alpha} S_r\right]\left[\rho_{r,n}\right]\left\{F_n\right\}}{\overline{C_{N_\alpha} S}\left(1 - \frac{x_{cp}}{x_{cg}}\right)} \tag{13}$$

Substituting equations (12) and (13) into equation (5), expressing the mass matrix and aerodynamic matrix in dimensionless form, and making permissible interchanges in subscripts, yields

$$\left\{F_n\right\} = q\overline{C_{N_\alpha} S}\left[\left[1\right] + \left\{\frac{m_r}{M}\right\}\left[\frac{x_{cp} - x_r}{x_{cg} - x_{cp}}\right] + \left[\frac{C_{N_\alpha} S_r}{\overline{C_{N_\alpha} S}}\right]\left\{1\right\}\left[\frac{x_r - x_{cg}}{x_{cg} - x_{cp}}\right]\right]\left[\frac{C_{N_\alpha} S_r}{\overline{C_{N_\alpha} S}}\right]\left[\rho_{r,n}\right]\left\{F_n\right\} \tag{14}$$

Equation (14) is of the familiar form of an eigenvalue problem; that is

$$\frac{1}{q\overline{C_{N_\alpha} S}}\left\{F_n\right\} = \left[A\right]\left\{F_n\right\} \tag{14a}$$

where $\frac{1}{q\overline{C_{N_\alpha} S}}$ is the eigenvalue and F_n is the eigenvector. The solution of equation (14) by matrix iteration techniques will converge on the dominant eigenvalue that yields the lowest value of $q\overline{C_{N_\alpha} S}$ from which the divergence dynamic pressure is derived.

The distribution of forces on the structure, when operating at the divergence dynamic pressure, is given by the eigenvector F_n.

If desired, the mode of divergence can be readily computed by elementary beam theory when the loads F_n and the zeroth element angle of attack v/u are known.

Generalized Static Margin

The static margin, that is, the distance from the center of gravity to the aerodynamic center, has long been used as a standard of stability for rigid vehicles. For the rigid structure the static margin is independent of the dynamic pressure q and can be determined in conventional ways. For the structure that is substantially deformed but not divergent, the variation of the static margin depends upon the instantaneous shape of the elastic curve. Except for the unique condition of equilibrium given by the eigenvalue solution of equation (14), there is no nontrivial homogeneous solution to the equations of equilibrium for nonoscillatory behavior. Only when the applied external loading (nonhomogeneous terms) is added to the problem is it possible to find other states of equilibrium. For such conditions a center of pressure and consequently a static margin can

be derived, but it will always be dependent upon the nonhomogeneous loading and therefore is not strictly a stability characteristic of the system itself.

A concept of a generalized static margin for either the rigid or flexible but stable vehicle will now be developed.

Consider changing the aerodynamic loading arbitrarily over a portion of the vehicle until the condition of divergence is encountered for the flight conditions of interest.

Varying the lift coefficient of a dominant lift panel at which a fin is located is particularly suitable and is normally chosen as the panel for arbitrary variation. In sketch B the idea is shown graphically.

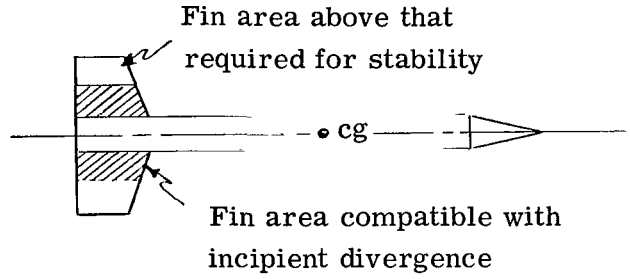

Sketch B

The shaded area represents the portion of the specific lift panel that, when considered in conjunction with other lift distributions, would result in neutral aeroelastic stability for the flight conditions under study. For the divergent mode of flight it can be seen from the associated equilibrium relationships given by equations (6) and (7) that the stabilizing moment about the center of gravity for the elastically deformed vehicle is zero. Hence, the static margin must be zero. It then follows that the stabilizing moment for the vehicle can be considered to result entirely from the lift on the panel above that associated with neutral stability. This marginal lifting surface is indicated in sketch B by the unshaded areas. An equation for an effective static margin based upon the preceding concept will be developed for the case of variation of the lift characteristics of the zeroth station.

For an elastically deformed vehicle the static margin can be stated in terms of the foregoing notation as follows:

$$x_{sm} = x_{cg} - \frac{\left[x_r\right]\left[C_{N_\alpha} S_r\right]\left\{\alpha_r\right\}}{\left[1\right]\left[C_{N_\alpha} S_r\right]\left\{\alpha_r\right\} + C_{N_\alpha} S_0 \alpha_0} \tag{15}$$

Rewrite this equation for a common denominator

$$x_{sm} = \frac{x_{cg}\left[1\right]\left[C_{N_\alpha}S_r\right]\left\{\alpha_r\right\} + x_{cg}C_{N_\alpha}S_0\alpha_0 - \left[x_r\right]\left[C_{N_\alpha}S_r\right]\left\{\alpha_r\right\}}{\left[1\right]\left[C_{N_\alpha}S_r\right]\left\{\alpha_r\right\} + C_{N_\alpha}S_0\alpha_0} \tag{16}$$

Let $C_{N_\alpha}S_0$ be divided into two parts, one part $C_{N_\alpha}S_{div}$, just equal to and compatible with that for which static instability for a rigid vehicle or aeroelastic divergence for an elastic vehicle would occur, and a second part $C_{N_\alpha}S_{mar}$ representing the margin of the zeroth-station aerodynamic coefficient; then, equation (16) can be written as

$$x_{sm} = \frac{x_{cg}\left(\left[1\right]\left[C_{N_\alpha}S_r\right]\left\{\alpha_r\right\} + C_{N_\alpha}S_{div}\alpha_0\right) - \left[x_r\right]\left[C_{N_\alpha}S_r\right]\left\{\alpha_r\right\} + x_{cg}C_{N_\alpha}S_{mar}\alpha_0}{\left[1\right]\left[C_{N_\alpha}S_r\right]\left\{\alpha_r\right\} + C_{N_\alpha}S_0\alpha_0} \tag{17}$$

For the vehicle that can be assumed essentially rigid, $\alpha_r \rightarrow \alpha_0$, and equation (17) reduces to

$$x_{sm,rig} = \frac{x_{cg}\left[1\right]\left[C_{N_\alpha}S_r\right]\left\{1\right\} + C_{N_\alpha}S_{div}x_{cg} - \left[x_r\right]\left[C_{N_\alpha}S_r\right]\left\{1\right\} + x_{cg}C_{N_\alpha}S_{mar}}{\overline{C_{N_\alpha}S}} \tag{18}$$

By the definition of $C_{N_\alpha}S_{div}$, however, the first three terms in the numerator of equation (18) for the rigid system are zero; that is

$$x_{cg}\left[1\right]\left[C_{N_\alpha}S_r\right]\left\{1\right\} + x_{cg}C_{N_\alpha}S_{div} - \left[x_r\right]\left[C_{N_\alpha}S_r\right]\left\{1\right\} = 0 \tag{19}$$

Consequently, equation (18) yields for the rigid system the expression

$$x_{sm,rig} = \frac{x_{cg}C_{N_\alpha}S_{mar}}{\overline{C_{N_\alpha}S}} \tag{20}$$

Also, as previously mentioned for significantly flexible systems when $C_{N_\alpha}S_{mar}$ approaches zero and divergence is reached, the static margin vanishes. Inspection of equation (17) will show that for the static margin to vanish, the same three functions corresponding to those of equation (19) must again equal zero, namely:

$$x_{cg}\left[1\right]\left[C_{N_\alpha}S_r\right]\left\{\alpha_r\right\} + x_{cg}C_{N_\alpha}S_{div}\alpha_0 - \left[x_r\right]\left[C_{N_\alpha}S_r\right]\left\{\alpha_r\right\} = 0 \tag{21}$$

The expression given by equation (21) is exact when $C_{N_\alpha}S_{mar}$ equals zero for either the completely rigid or the divergent vehicle. Hence, it is suggested that even for non-divergent, substantially elastic structures, the sum of the same first three functions in the numerator of the right-hand member of equation (17) be assumed zero. Such an assumption leads to

$$x_{sm} = \frac{x_{cg}C_{N_\alpha}S_{mar}}{\left[1\right]\left[C_{N_\alpha}S_r\right]\left\{\frac{\alpha_r}{\alpha_0}\right\} + C_{N_\alpha}S_0} \tag{22}$$

For substantially rigid systems, the column matrix α_r/α_0 approaches unity, and equation (22) approaches the rigid-body relationship given by equation (20). For nearly divergent systems, the numerator of equation (22) approaches zero and even though α_r/α_0 varies somewhat from unity, the consequence of assuming it to be unity is acceptable in view of the quotient. Hence, equation (22) reduces to the form of equation (20) and is suggested as an expression for the generalized static margin for the flexible vehicle:

$$x_{gsm} = \frac{x_{cg}C_{N_\alpha}S_{mar}}{\overline{C_{N_\alpha}S}} \tag{23}$$

This concept of a generalized static margin can be stated in words. It is the rigid-body moment about the center of gravity associated with the difference between the initial and modified normal-force-coefficient distribution divided by the total force associated with the initial normal-force-coefficient distribution.

Equation (23) is an exact expression for the rigid system (same as eq. (20)) and properly vanishes for the case of divergent flight behavior. For cases between these limits, it will approximately account for the degenerating effects of flexibility on stability. It is therefore offered as a measure of stability to be used in a manner somewhat analogous to the conventional rigid-body static margin. The parameter $C_{N_\alpha}S_{mar}$ is obtained by trial and error solutions of equation (14) for different values of $C_{N_\alpha}S_0$ until $\frac{q}{q_{div}} = 1$. Then,

$$C_{N_\alpha}S_{mar} = C_{N_\alpha}S_0 - C_{N_\alpha}S_{div} \tag{24}$$

For some vehicle configurations with large fins on intermediate stages, the local lift of such fins provides sufficient intermediate support to produce one or more inflection points in the divergent mode shape. In unusual cases of this kind a $C_{N_\alpha}S_{div}$ cannot

be obtained by reducing the $C_{N_\alpha}S_0$, since the divergence dynamic pressure will be found to increase with decreases in $C_{N_\alpha}S_0$. Conversely, an increase in $C_{N_\alpha}S_0$ will produce a decrease in q_{div}. In essence, for vehicles of this behavior, aeroelasticity is found to improve stability rather than to be a degenerative influence. The foregoing development of the concept of x_{gsm} has been offered as an index of the degenerative influence of aeroelasticity on the conventional static margin. It is therefore concluded that for the generalized static margin to fulfill this prime objective, it be considered applicable only to vehicles where a decrease in q_{div} is experienced for a decrease in $C_{N_\alpha}S_0$.

THEORETICAL CONSIDERATIONS

Equations (14) and (14a) are eigenvalue problems that yield the lowest divergence dynamic pressure at which aeroelastic divergence occurs in unguided launch vehicles. Equation (23) provides a means for obtaining a generalized static margin for the flexible launch vehicle that is comparable to the traditional rigid-body stability criterion.

Significance of Divergence Dynamic Pressures

The mass and aerodynamic characteristics contained in the A matrix of equation (14a) are associated with a particular flight time and Mach number. Generally, the divergence dynamic pressure obtained from equation (14) will differ from the nominal dynamic pressure associated with the programed trajectory. To use this difference as an indication of a margin of stability does not require any further definition as to the probable altitude, Mach number, velocity-time combinations at which such a value of dynamic pressure can be obtained. If the computed dynamic pressure is used in such a manner, a margin of stability based on q alone is being found for the constraints that all other pertinent parameters affecting the solutions are held invariant.

Such a solution does not determine the actual time and conditions in a trajectory where aeroelastic divergence would occur. When it is assumed that such a condition could occur within the applicable trajectory for a given vehicle staging, then it is necessary to iterate on solutions of the type given by equation (14). The iteration would require new aerodynamic and mass distributions for the vehicle characteristics associated with the preceding estimate of the divergence dynamic pressure. The process should converge to sufficient accuracy in a few solutions. Such a solution will yield a dynamic pressure compatible with time, altitude, velocity, mass, and aerodynamic properties for which it was obtained. The iterative procedure is hardly necessary in achieving the principal purpose from the subject analysis of computing stability criteria. Iteration, however, is essential in attempting to show correlation between computed and observed results of aeroelastic divergence.

Influence Coefficients

The influence coefficients, defined as $\rho_{r,n}$, are essential to the solutions of equation (14). In reference 5 slope influence coefficients are developed in detail and will suffice for the present analysis. In the referenced paper, the influence coefficients are treated as a combination of those resulting from beam flexure and those due to joint rotations. The joint rotations are determined on the assumption that the rotation at the joint is defined as a linear function of the local moment. Some useful empirical data for determining appropriate joint rotation spring constants, in the absence of measured values, are given in reference 6. Experience has shown that joints can frequently cause severe reduction in the aeroelastic stability characteristics for launch vehicles of conventional fabrication.

The influence coefficients of reference 5 do not include the effects of shear deformation or axial load contributions to flexure. Whereas the formulation of the present analysis precludes consideration of axial effects on bending, the results will readily accommodate shear effects. The deformation due to shear can be accounted for in computing the influence coefficients and affects the stability solution only insofar as it alters the values of the influence coefficients. For conventional vehicle structures, shear deformation can be considered as a secondary influence on divergence.

Suitability for Digital Computers

The organization of the aeroelastic divergence problem into the classical eigenvalue-eigenfunction form makes it ideal for programing on digital computers. Solutions of equations of the general form of equation (14a) are available as library routines at most large computer installations. Furthermore, the coefficients of the A matrix of equation (14a) are shown in equation (14) to be simple matrix additions and multiplications of functions of known vehicle characteristics. It should also be noted that solutions of equation (14) by manual computing remain feasible for matrices of moderate order (that is, of the order 10×10).

NUMERICAL CONSIDERATIONS

The aeroelastic divergence analysis, as derived in the foregoing section on "Theory," is dependent upon an appropriate numerical representation of the vehicle stiffness, mass, and aerodynamic characteristics as well as trajectory parameters. Typical and essential input data for accomplishing an analysis, along with a display of results and associated comments, are discussed in this section.

Input Characteristics

In table I a tabulation of the flexural stiffness coefficient EI is presented that is valid for the NASA research vehicle RAM III. Also, the data of table I are displayed graphically in figure 1. Note that these data are highly descriptive and account in detail for the significant variations in stiffness throughout the structure. The discontinuities seen in the figure are accounted for in table I by simply recording both quantities for their common x values. In table II appropriate joint rotation spring constants κ_u and their x positions c_u are shown for the joint geometries used in the RAM III fabrication. These data were derived by the procedures given in reference 6. The data of tables I and II provide the essential information for deriving the required influence coefficients $\rho_{r,n}$ by the method set forth in reference 5. In table III the weight distribution for the RAM III vehicle is tabulated and a graph of the data is supplied as figure 2. These data are valid for the time of flight corresponding to Mach 4, at which the maximum dynamic pressure is encountered. It is at this time in flight that the aeroelastic divergence problem generally is most acute.

In figure 3 a graph of the distributed aerodynamic normal-force-coefficient derivative $S\frac{dC_{N_\alpha}}{dx}$ is submitted for Mach 4 for the RAM III vehicle. The distributed or running aerodynamic loading along the body of the vehicle is obtained by the product of the aerodynamic normal-force-coefficient derivative, the local angle of attack, and the dynamic pressure of the airstream. Data such as are given in figure 3 can be derived from techniques such as those of references 7, 8, and 9. In reference 9, Muraca gives a very comprehensive compilation of experimentally obtained distributed normal-force-coefficient derivatives applicable to typical launch-vehicle configurations. These data have been reduced from numerous wind-tunnel tests and yield reliable descriptions for distributed aerodynamics for rather complex geometries involving cones, cylinders, frustums, ogives, and boattail components. Such procedures as are employed in references 7, 8, and 9 are widely used. However, for sophisticated vehicles involving large investments, it is believed that wind-tunnel pressure tests of specific geometries are justified. The complexity of pressure models, costs of tunnel operations, and the extensive data reduction preclude such tests for minor developments.

Along with the body normal-force distributions, fin-lift data are essential to the aeroelastic solution. In figure 4, aerodynamic characteristics of the RAM III fin necessary to the analysis are furnished, along with needed trajectory data for providing the Mach number and dynamic-pressure relationships with time. Before the effectiveness of fin panels can be determined, it is necessary to consider decreased effectiveness due to downwash from upper stage fins and to include body-fin interference effects.

Useful body-fin interference characteristics are obtainable from the theoretical procedures of Pitts, Nielsen, and Kaattari in reference 10. Also, helpful fin-lift data

based on theoretical and experimental methods are presented in the 1963 revision of the USAF Stability and Control DATCOM (ref. 11).

Discrete Representation

In the section on "Theory" the formulation was founded upon local lifting panels and discrete mass representation of the continuous vehicle structure. Also, a single x coordinate was used at each station to define both the center of the panel lift and the center of the mass. In this method of discrete representation, it is impossible to locate rigorously all the centers of pressure of the panels at the centers of gravity of their corresponding masses. An adequate approximation toward achieving concentricity can be effected by use of a large number of stations and by using discretion when establishing the station boundaries. The station boundaries for the lift panels, in general, must be different from those used in determining the masses.

The boundaries for the lift panels and the separate boundaries for the masses are illustrated in figure 5.

The centers of pressure and centers of gravity of the various stations are illustrated in the figure and the mass and aerodynamic centers closely approach coincidence for most of the significant points. It has been found that the best results are obtained by forcing concentricity at the principal lift stations (such as station 4) and letting the major discrepancy occur at a so-called "makeup station" (station 2 in the figure). Note the lack of coincidence between the center of gravity and center of pressure of the makeup station. In some cases it may prove necessary to use a zero area at a station to produce better agreement between the location of centers of pressure and centers of gravity.

In figure 6 the analogous discrete system for the RAM III vehicle is shown. Twenty-three ($p = 23$) discrete stations were used in the illustrated case, which is typical of many other applications. Use of a significantly larger number of stations, in general, offers little advantage, and good results have been obtained with as little as eight stations. The position of the zeroth station (i.e., origin of x) for the RAM III was taken at the center of pressure of the fin assembly. This point represents a position of a principal lift station because of the large concentrated aerodynamic force. The data of figure 6, obtained by discrete representation of the mass and aerodynamic distributions of figures 2 and 3, are directly usable in the solution of equation (14).

Output

The significant output from the solution of equation (14) is the eigenvalue $\frac{1}{q\overline{C_{N_\alpha}S}}$ from which the divergence dynamic pressure is obtained. If λ is the eigenvalue

obtainable from the matrix iteration of equation (14), the divergence dynamic pressure is then

$$q_{div} = \frac{1}{C_{N_\alpha} S \lambda}$$

Divergence q ratio as a function of $C_{N_\alpha}S_0$.- The significant variations in the RAM III stability index q/q_{div} with variation in $C_{N_\alpha}S_0$ (the zeroth station aerodynamic coefficient) are illustrated in figure 7 for the flight conditions at Mach 4. The quantity $C_{N_\alpha}S_0$ is composed of normal-force contributions of both body and fin, but for most conventional launch-vehicle geometries, it is predominantly due to the fin contributions. Thus, the variations of the data of figure 7 could be considered as the direct result of fin changes. The solid-line curve of q/q_{div} as a function of $C_{N_\alpha}S_0$ goes asymptotically vertical at the value of $C_{N_\alpha}S_0$ of 1070 in^2/radian (0.6903 m^2/radian), which is the value associated with a zero rigid-body static margin. The divergence normal-force coefficient at the zeroth station for the flexible vehicle is 1320 in^2/radian (0.8516 m^2/radian), which is the value at which aeroelastic divergence occurs $\left(\frac{q}{q_{div}} = 1\right)$. Also, the $C_{N_\alpha}S_0$ value of 2060 in^2/radian (1.329 m^2/radian), which is commensurate with a static margin of 1 diameter for a rigid structure, is indicated in the figure on the abscissa scale. The nominal design value of $C_{N_\alpha}S_0$ for the RAM III vehicle is 2475 in^2/radian (1.597 m^2/radian) and is noted by the cross on the curve. It is evident that small reductions in fin lift when $C_{N_\alpha}S_0$ is less than 1600 in^2/radian (1.032 m^2/radian) result in severe reductions in the margins against aeroelastic divergence. It is obviously undesirable for a design to be established for which the nominal $C_{N_\alpha}S_0$ is on the part of the curve of figure 7 with a high negative slope. Small uncertainties in fin characteristics could result in divergent flight behavior when the nominal design is near the vertical asymptote of the curve.

It is equally apparent from the solid curve of figure 7 that on the left end of the curve stability is rapidly improved by increasing the first-stage fin-lift contributions. Since the curve also becomes asymptotic to the abscissa, only trivial gains can be accomplished in the regions to the right where the slope of $\frac{q}{q_{div}} \to 0$. Attempts to increase the margin of stability by increasing $C_{N_\alpha}S_0$ in the region of low slope are seldom justified because of the resulting excessively large fins. Fin-flutter problems, as well as penalties associated with increased drag and weight, may be introduced. For designs showing an inadequate margin against divergence and exhibiting a low slope of curves of q/q_{div} as a function of $C_{N_\alpha}S_0$, other corrective measures must be used. Such a condition is generally traceable to excessive flexibility in the forward portion of the vehicle and cannot be rectified by increasing first-stage fin areas, however large. For this type of

problem, increases in second-stage fin areas or improvement in the structural stiffness, or both, are helpful. The analyst should be alert to the fact that when second-stage fin sizes are increased, the associated decrease in the first-stage fin effectiveness due to downwash must be considered.

The remedial action of increasing first-stage fin areas was used in the illustrated case of the RAM III vehicle, since a divergence problem was indicated for the configuration in the conceptional design.

The dashed curve of figure 7 represents the variation of q/q_{div} with changes in fin-lift coefficients for the artificial case of extreme structural stiffness; i.e., $EI \to \infty$. This curve has been added to show the comparative relationships between analyses for the rigid and flexible bodies when presented in terms of the divergence dynamic pressure parameter. For the rigid body, the q/q_{div} ratio approaches a discontinuity (or step) at a value of $C_{N_\alpha}S_0$ compatible with a zero rigid-body static margin. For the vehicle assumed extremely rigid and possessing positive static stability, the divergence dynamic pressure approaches infinity, and consequently, q/q_{div} approaches zero.

Generalized static margin.- In figure 8 the generalized static margins for the RAM III vehicle assumed rigid and also considered flexible are compared for a range of $C_{N_\alpha}S_0$. The generalized static margins for the vehicle were determined by the method of equation (23). It is interesting to note that when the boundary between stability and instability is encountered for a $C_{N_\alpha}S_0$ of 1320 in^2/radian (0.8516 m^2/radian), the rigid-body analysis shows a static margin of 9 inches (0.23 m). It is not uncommon for typical solid-propellant multistage vehicles to experience reductions in static margin of the order of 1 maximum body diameter because of flexibility. For example, in reference 3, a reduction in static margin of 2 maximum body diameters is recorded. These data can be interpreted to mean that failure to consider flexibility effects in assessing the vehicle's stability can lead to nonconservative conclusions.

STABILITY CRITERIA

The authors' experiences have shown that, for significantly flexible structures, an adequate margin against aeroelastic divergence can be assured by maintaining the q/q_{div} ratio equal to or less than 1/2. This constraint is a necessary but not sufficient criterion. For flexible vehicles it is the controlling criterion, but for rigid vehicles it is insufficient and can be misleading. For example, just to the right of the dashed curve in figure 7 for the highly rigid vehicle, an extreme margin against aeroelastic divergence is indicated by the nearly zero q/q_{div}. However, a small reduction in $C_{N_\alpha}S_0$ attributable to aerodynamic uncertainties would quickly result in a static stability failure (i.e., $x_{sm} < 0$). Consequently, in order to safeguard structures within the extremes of

flexibility and rigidity, dual constraints are necessary. Both the traditional rigid-body static-margin criterion of maintaining a margin of at least 1 maximum body diameter and the provision that q/q_{div} be less than 1/2 have proven useful as cocriteria for stability. The static-margin criterion will predominate for rigid vehicles and the q/q_{div} criterion will predominate for the flexible vehicles.

In addition, the traditional rigid-body criterion of maintaining a static margin of 1 maximum body diameter or greater has shortcomings when exceedingly slender systems are involved. To protect against this contingency, an additional constraint requiring that the rigid-body static margin be not only 1 maximum body diameter or greater but also not less than 1/15 the vehicle length is useful. The foregoing criteria can be summarized in equation form as follows:

$$\frac{q}{q_{div}} \leqq \frac{1}{2}$$

$$\frac{L}{15} \leqq x_{sm,rig} \geqq D_{max}$$

In figure 7, it can be seen, for the illustrated RAM III vehicle, that for the designed $C_{N_\alpha}S_0$, the q/q_{div} ratio is 0.48, just below the limit value. The RAM III, for the study conditions at Mach 4 has a rigid-body static margin $x_{sm,rig}$ of 41 inches (1.04 m) which is 1.32 maximum body diameters. Also, the x_{sm} is 1/12 the length and thereby greater than the L/15 minimum.

Observance of the criterion $\frac{q}{q_{div}} \leqq \frac{1}{2}$ provides a twofold advantage. In addition to maintaining a margin for providing for uncertainties in the aeroelastic parameters, it also limits the aeroelastic magnification of external loading. As q/q_{div} becomes large and instability is approached, the effects of externally applied loads are magnified in a sense similar to the resonant or near resonant response of a vibrating system. In fact, the two problems are mathematically similar. The large load magnifications that occur in systems with high ratios of q/q_{div} are revealed in transient-load analyses for flexible vehicles which are beyond the scope of this paper. However, maintaining a conservative ratio of q/q_{div} will preclude unnecessary weight penalities that would arise as a result of large aeroelastic load magnifications on the less stable but otherwise similar configurations.

In the previous discussion on the derivation for the generalized static margin x_{gsm}, it was stated that it could be used as a measure of stability. Some data on the relationships between the maximum ratios of q/q_{div} and the related static margins and generalized static margins are provided in figure 9. In all cases the values of x_{gsm} have been calculated by equation (23) with the C_{N_α} variation taken on the zeroth panel.

The heavy horizontal lines in figure 9(a) designate the reduction in static margin x_{sm}, due to flexibility with the right-hand ends denoting the magnitudes of static margin when the structure is assumed rigid and the left-hand end denoting the values of x_{gsm} when the same structures are considered flexible. The static margins are rendered dimensionless by expressing them in ratio to the maximum diameter of the body of the respective configurations studied. It is seen from figure 9(a) that for increasing values of q/q_{div} there tends to be a larger difference between x_{sm} and x_{gsm}, as would be expected. Also, the calibers of static margin for the rigid vehicle are not indicative of the reduction in static margin due to flexibility. Thus, it is seen that a large rigid-body static margin does not insure adequate aeroelastic stability.

The vehicles for which both q_{div} and x_{gsm} data are shown were widely varied in configuration, staging, and trajectory characteristics. When more than one data point is shown for a given vehicle, these points are either for different stages or for different Mach numbers during flight. The vehicle of curve 1 was not flown in the configuration analyzed, partly because of its marginal aeroelastic characteristics; however, with modifications that led to acceptable stability, it has shown consistent performances. A correlation between the q_{div} and x_{gsm} on the modified configuration is not available.

The q/q_{div} values displayed for vehicle 2 are near the limits set by the foregoing stability criterion. The case where the largest static margin shift is experienced is associated with flight conditions at the maximum dynamic pressure. At both flight conditions, vehicle 2, although of adequate reliability, has exhibited performances that imply minimum acceptable stability characteristics.

Vehicles 3 and 4 have been adequate in performance as regards aeroelastic stability. Vehicle 5 was a conceptional design that was carefully engineered but never funded for flight hardware. Vehicle 6 is for a typical three-stage configuration for which hardware is now being procured. Vehicle 7 is a four-stage flight vehicle which has exhibited excellent stability characteristics. The data of vehicle 8 as yet have not been flight proven. Vehicles 9 and 10 are known to have experienced aeroelastic divergence for which details are documented in reference 3. The q/q_{div} value of 0.82 for vehicle 9 was computed for conditions associated with the observed failure, whereas the q/q_{div} value of 0.94 was computed for conditions just subsequent to failure. The q/q_{div} value of 0.62 for vehicle 10 is associated with flight conditions at Mach 3.2 whereas the q/q_{div} value of 0.92 is associated with conditions just prior to failure, which was observed to occur at Mach 4. The data for vehicles 11 and 12 are flight qualified for their adequate aeroelastic performances. The data point for vehicle 12 is omitted in figure 9(a) since it falls outside of the limits of the abscissa. The x_{gsm}/D and x_{sm}/D values for vehicle 12 are 3.7 and 4.7, respectively, at a q/q_{div} ratio of 0.26.

The data of figure 9(a) are also submitted in the format of figure 9(b). An apparent correlation is seen between the q/q_{div} and $x_{gsm}/x_{sm,rig}$ ratios. A second-order polynomial was fitted to the data by the method of least squares and, in addition, two added known constraints were imposed; namely, that $\frac{x_{gsm}}{x_{sm,rig}} = 0$ when $\frac{q}{q_{div}} = 1$ and $\frac{x_{gsm}}{x_{sm,rig}} = 1$ when $\frac{q}{q_{div}} = 0$. This function is shown in the figure by the solid line.

The proposed limiting value of q/q_{div} is also shown by the horizontal dashed line. The areas to the top and left of the two curves are suggested as regions of unsuitable combinations of q/q_{div} and $x_{gsm}/x_{sm,rig}$. The triangular area on the lower right bounded by the polynomial and the $\frac{q}{q_{div}} = 0.5$ curves is considered a region of favorable parameters. The intercept of the two boundary curves occurs at $\frac{q}{q_{div}} = 0.5$ and $\frac{x_{gsm}}{x_{sm,rig}} = 0.6$. The correlation of data on the divergence dynamic pressures and generalized static margins indicate that restricting the ratio $x_{gsm}/x_{sm,rig}$ to the intercept value or greater $\left(\frac{x_{sm}}{x_{sm,rig}} \geqq 0.6\right)$ will provide a realistic constraint on the generalized static margin that will preclude aeroelastic divergence. This criterion could be used cautiously in place of the criterion $\frac{q}{q_{div}} \leqq 0.5$ and in conjunction with the foregoing recommended rigid body criteria. It simply means that a 40-percent reduction in the traditional rigid-body static margin due to flexibility is tolerable.

CONCLUDING REMARKS

The equations essential to performing aeroelastic divergence analyses and the necessary input data for facilitating a solution, as well as typical output results, have been presented. Some problems associated with reducing a continuous system to an analogous discrete system are considered. A detailed discussion is included on the effects of fin normal force on aeroelastic stability.

The divergence dynamic pressure and a concept of a generalized static margin are discussed as measures of aeroelastic stability. In particular, the meanings of these measures are considered for vehicles encompassing the extremes of either flexibility or rigidity or of high slenderness. Also, the relationship between the traditional rigid-body static margin and the generalized static margin is considered.

Suggested criteria that are considered necessary and sufficient for stability are presented. It is believed that maintaining the suggested criteria not only would provide

a desirable margin against divergence but also would effectively limit large aeroelastic magnifications of the effects of applied loads.

Langley Research Center,
National Aeronautics and Space Administration,
Langley Station, Hampton, Va., October 19, 1965.

REFERENCES

1. Bisplinghoff, Raymond L.; and Ashley, Holt: Principles of Aeroelasticity. John Wiley & Sons, Inc., c.1962.

2. Arbic, Richard G.; White, George; and Gillespie, Warren, Jr.: Some Approximate Methods for Estimating the Effects of Aeroelastic Bending of Rocket-Propelled Model-Booster Combinations. NACA RM L53A08, 1953.

3. Thomson, K. D.: The Aero-Elastic Divergence of Slender Multi-Stage Test Vehicles. Tech. Note HSA-93, Weapons Res. Estab., Australian Defence Sci. Serv., Nov. 1962.

4. Mechtly, E. A.: The International System of Units – Physical Constants and Conversion Factors. NASA SP-7012, 1964.

5. Alley, Vernon L., Jr.; and Gerringer, A. Harper: A Matrix Method for the Determination of the Natural Vibrations of Free-Free Unsymmetrical Beams With Application to Launch Vehicles. NASA TN D-1247, 1962.

6. Leadbetter, Sumner A.; Alley, Vernon L., Jr.; Herr, Robert W.; and Gerringer, A. Harper: An Experimental and Analytical Investigation of the Natural Frequencies and Mode Shapes of a Four-Stage Solid-Propellant Rocket Vehicle. NASA TN D-1354, 1962.

7. Phythian, J. E.; and Dommett, R. L.: Semi-Empirical Methods of Estimating Forces on Bodies at Supersonic Speeds. J. Roy. Aeron. Soc., vol. 62, no. 571, July 1958, pp. 520-524.

8. Syvertson, Clarence A.; and Dennis, David H.: A Second-Order Shock-Expansion Method Applicable to Bodies of Revolution Near Zero Lift. NACA Rept. 1328, 1957. (Supersedes NACA TN 3527.)

9. Muraca, Ralph J.: An Empirical Method for Determining Static Distributed Aerodynamic Loads on Axisymmetric Multistage Launch Vehicles. NASA TN D-3283, 1966.

10. Pitts, William C.; Nielsen, Jack N.; and Kaattari, George E.: Lift and Center of Pressure of Wing-Body-Tail Combinations at Subsonic, Transonic, and Supersonic Speeds. NACA Rept. 1307, 1957.

11. Douglas Aircraft Co., Inc.: USAF Stability and Control Datcom. Aeron. Systems Div., U.S. Air Force, Oct. 1960. (Rev. July 1963.)

TABLE I.- FLEXURAL STIFFNESS DISTRIBUTION OF RAM III VEHICLE

x/L	EI/EI_{max}	x/L	EI/EI_{max}	x/L	EI/EI_{max}
0.0	1.0000	0.4481	0.1310	0.7368	0.0382
.0202	1.0000	.4481	.1203	.7428	.0382
.0404	1.0000	.4570	.1182	.7428	.0369
.0606	1.0000	.4643	.1176	.7509	.0369
.0706	1.0000	.4844	.1155	.7569	.0369
.0807	1.0000	.4945	.1143	.7670	.0369
.1009	1.0000	.5046	.1123	.7771	.0369
.1212	1.0000	.5248	.1096	.7822	.0369
.1312	1.0000	.5288	.1091	.7872	.0369
.1413	1.0000	.5430	.1069	.7973	.0369
.1615	1.0000	.5430	.0856	.8074	.0369
.1817	1.0000	.5551	.0856	.8124	.0369
.1918	1.0000	.5652	.0856	.8175	.0369
.2019	1.0000	.5753	.0856	.8286	.0369
.2220	1.0000	.5854	.0856	.8286	.1019
.2422	1.0000	.5955	.0856	.8353	.1019
.2473	1.0000	.6056	.0856	.8353	.0773
.2624	1.0000	.6156	.0856	.8377	.0773
.2826	1.0000	.6257	.0856	.8478	.0773
.2977	1.0000	.6358	.0856	.8579	.0773
.3028	1.0000	.6459	.0856	.8639	.0773
.3230	1.0000	.6560	.0856	.8639	.0610
.3431	1.0000	.6641	.0856	.8680	.0561
.3482	1.0000	.6641	.1283	.8780	.0428
.3633	1.0000	.6762	.0749	.8881	.0294
.3835	1.0000	.6863	.0561	.8902	.0267
.4037	1.0000	.6883	.0535	.8982	.0241
.4178	1.0000	.6883	.0382	.9083	.0187
.4178	.1176	.6964	.0382	.9184	.0134
.4239	.1203	.7004	.0382	.9204	.0123
.4340	.1243	.7065	.0382	.9204	.0267
.4441	.1283	.7166	.0382	.9285	.0267
		.7267	.0382	.9356	.0267

$EI_{max} = 37.4 \times 10^9$ lb-in^2 $\left(107 \times 10^6 \text{ N-m}^2\right)$

L = 495.4 in. (12.58 m)

TABLE II.- JOINT ROTATION CONSTANTS

Description	Classification	c_u		κ_u	
		in.	m	rad/in-lbf	rad/m-N
Bolted	Moderate (+)	19.78	0.502	1.5×10^{-9}	13.28×10^{-9}
Heavy, bolted	Excellent (+)	204.29	5.189	.01	.0885
Riveted to inner ring	Moderate (+)	206.94	5.256	1.5	13.28
Threaded diaphragm	Good (-)	221.82	5.634	.3	2.655
Light flange, riveted	Moderate (+)	268.05	6.808	2.0	17.70
Bolted	Excellent (+)	328.90	8.354	.04	.3540
Lapped, rivets	Moderate-poor	330.99	8.407	4.0	35.40
Lapped, rivets	Moderate (+)	338.5	8.598	2.5	22.13
Threaded diaphragm	Good	340.0	8.636	.8	7.081
Screwed to inner ring	Moderate-good	367.2	9.327	2.0	17.70
Screws, lapped	Moderate (-)	410.5	10.43	10.0	88.51

TABLE III.- WEIGHT DISTRIBUTION OF RAM III VEHICLE

Valid for flight time at Mach 4 (maximum dynamic pressure)

Span of x,		Weight per in. (m)	
in.	m	lbf/in.	N/m
-18.18 to -10.0	-0.462 to -0.254	27.5	4816
-10.0 to .0	-.254 to .0	18.0	3152
.0 to 10.0	.0 to .254	18.7	3275
10.0 to 20.0	.254 to .508	18.3	3205
20.0 to 50.0	.508 to 1.270	7.90	1384
50.0 to 90.0	1.270 to 2.286	8.00	1401
90.0 to 140.0	2.286 to 3.556	8.10	1419
140.0 to 160.0	3.556 to 4.064	8.20	1436
160.0 to 170.0	4.064 to 4.318	8.80	1541
170.0 to 180.0	4.318 to 4.572	24.7	4326
180.0 to 200.0	4.572 to 5.080	9.40	1646
200.0 to 210.0	5.080 to 5.334	13.4	2347
210.0 to 220.0	5.334 to 5.588	6.69	1172
220.0 to 230.0	5.588 to 5.842	11.4	1996
230.0 to 240.0	5.842 to 6.096	6.60	1156
240.0 to 250.0	6.096 to 6.350	5.70	998
250.0 to 260.0	6.350 to 6.604	4.60	806
260.0 to 270.0	6.604 to 6.858	16.7	2925
270.0 to 330.0	6.858 to 8.382	32.2	5639
330.0 to 340.0	8.382 to 8.636	26.5	4641
340.0 to 350.0	8.636 to 8.890	4.70	823
350.0 to 360.0	8.890 to 9.144	3.40	595
360.0 to 370.0	9.144 to 9.398	12.5	2189
370.0 to 410.0	9.398 to 10.414	19.2	3362
410.0 to 420.0	10.414 to 10.668	12.7	2224
420.0 to 440.0	10.668 to 11.176	5.00	876
440.0 to 450.0	11.176 to 11.430	3.00	525
450.0 to 477.2	11.430 to 12.121	.735	129

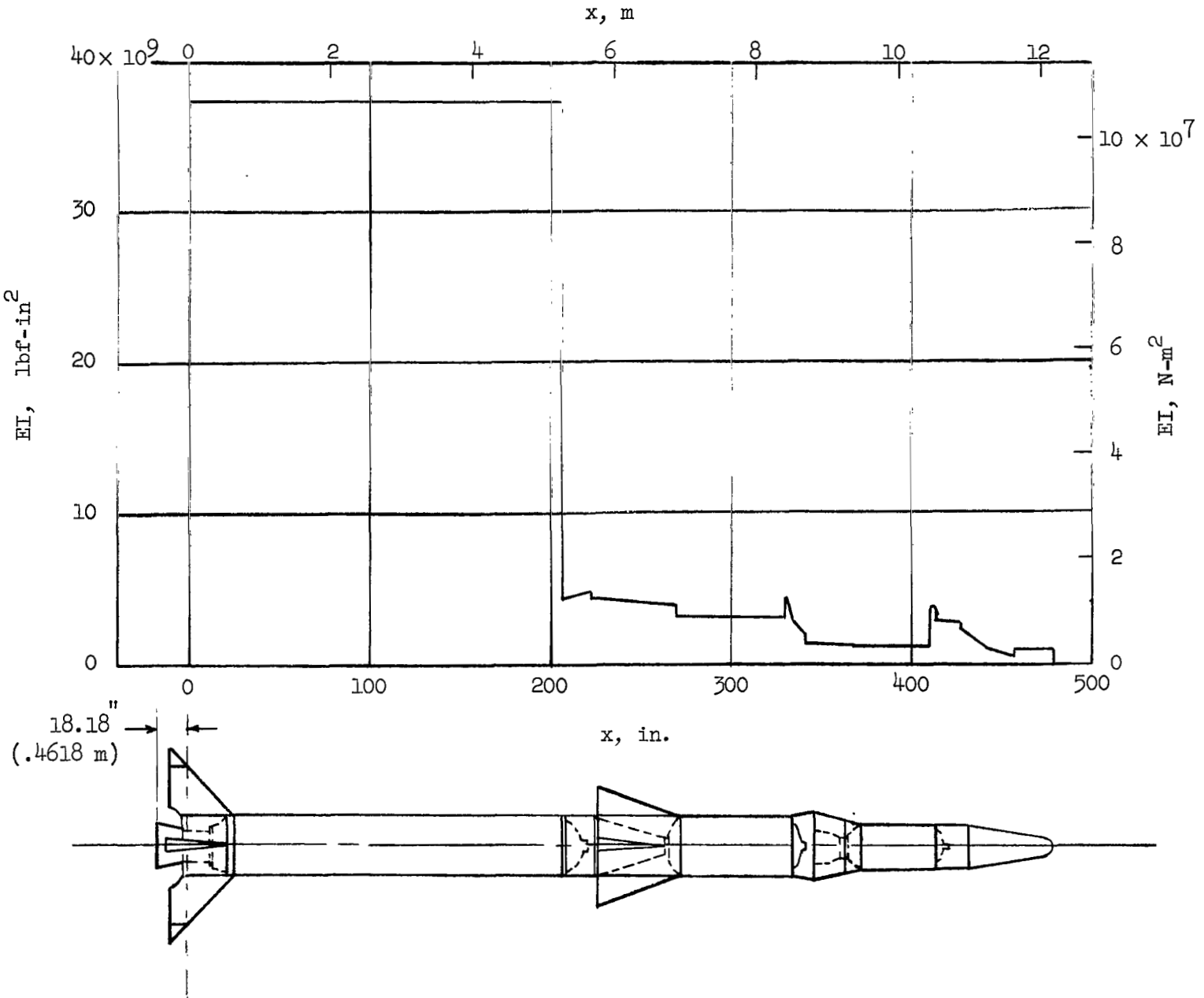

Figure 1.- EI distribution for RAM III vehicle.

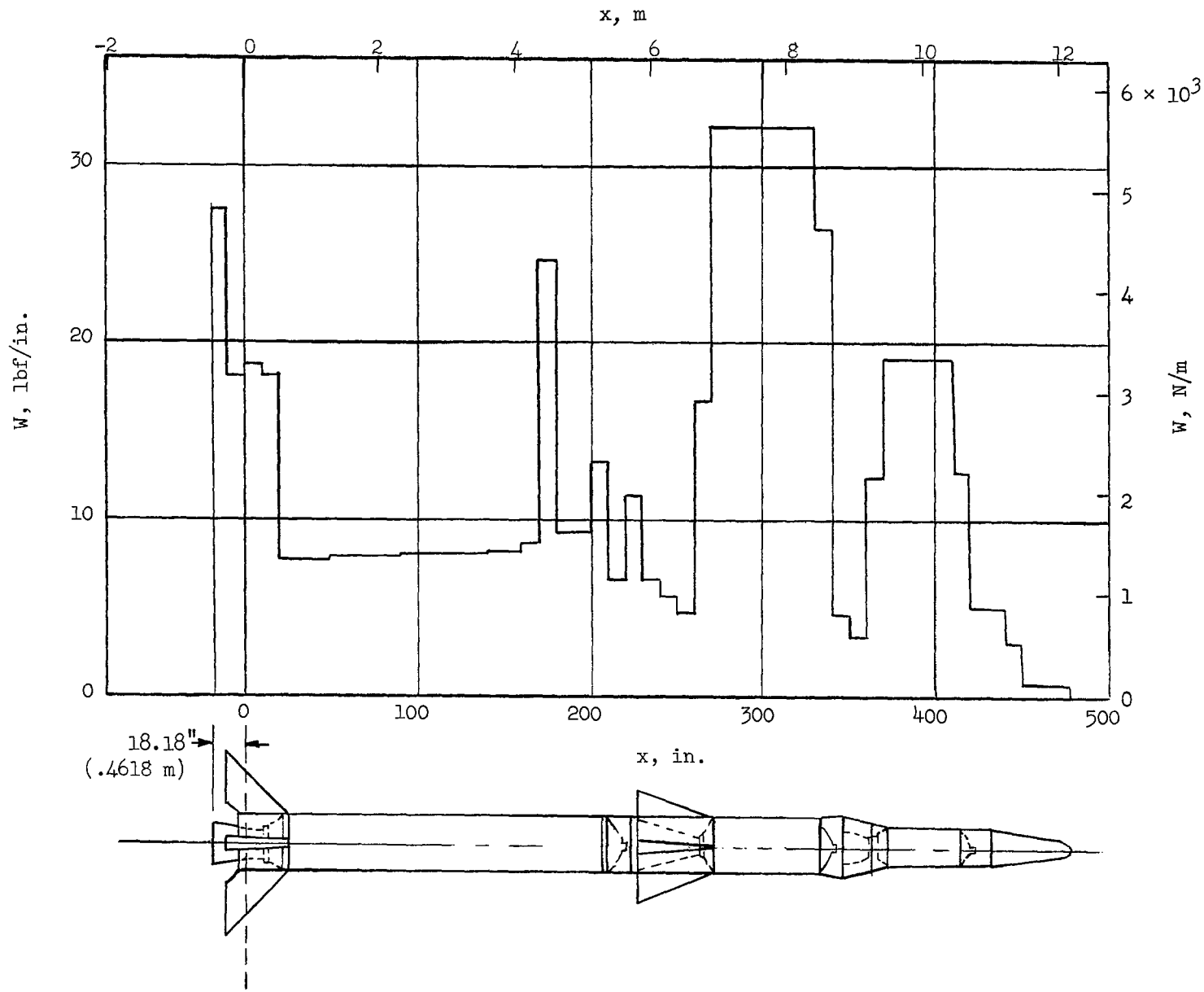

Figure 2.- Weight per inch (meter) curve for RAM III vehicle at Mach 4.

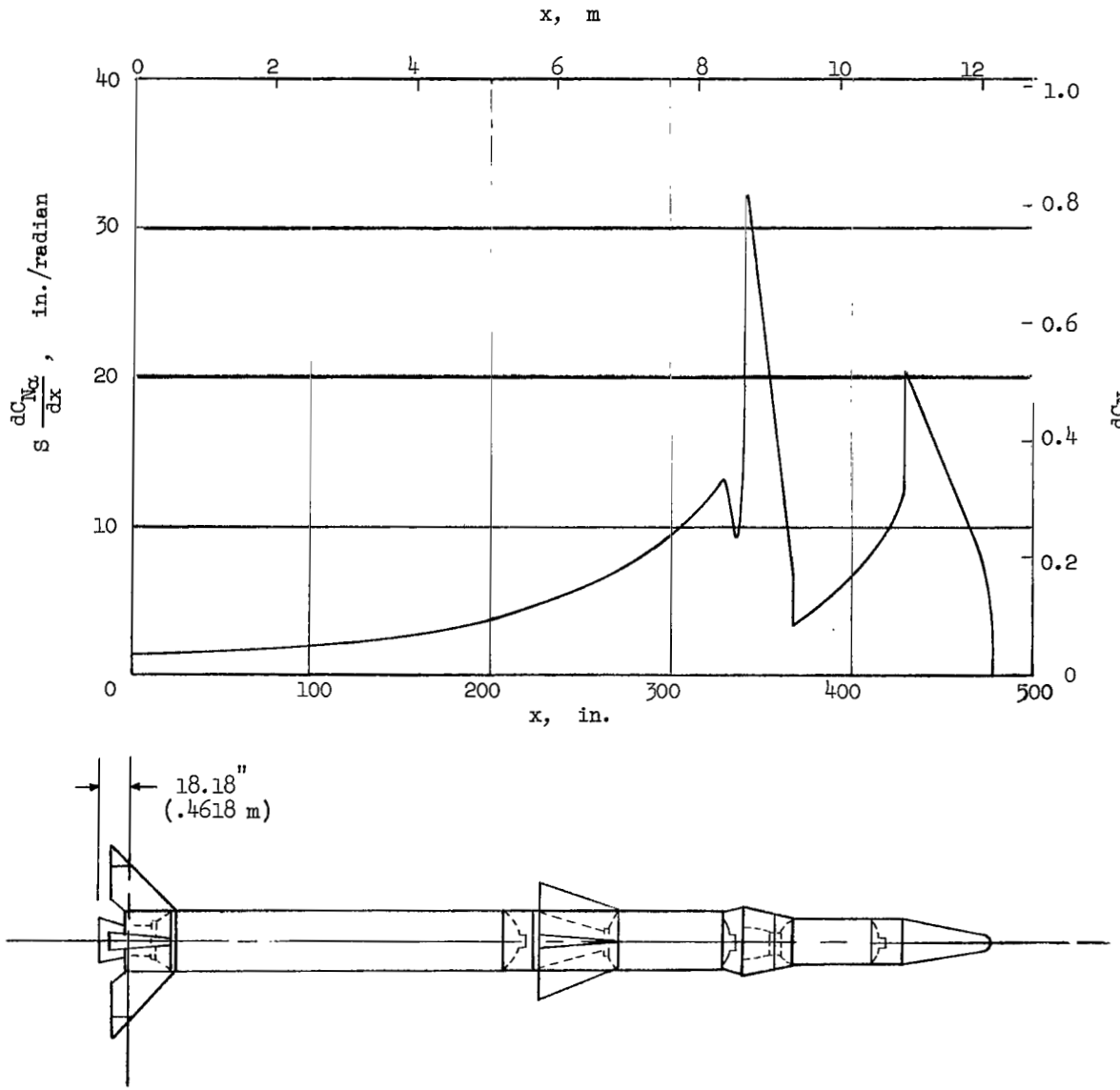

Figure 3.- Distributed normal-force-coefficient slope for RAM III vehicle at Mach 4.

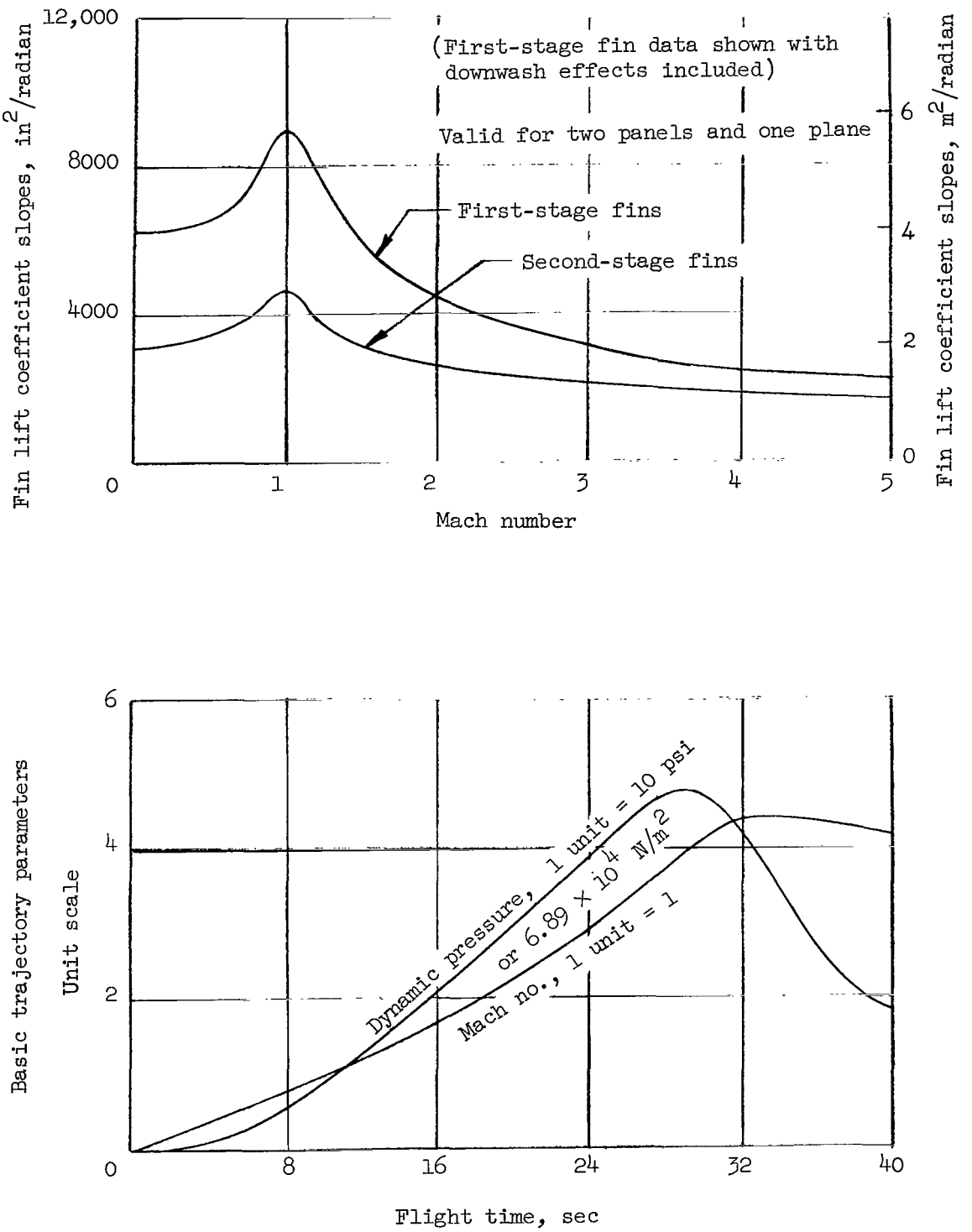

Figure 4.- Fin lift coefficient slopes and basic trajectory parameters for RAM III vehicle.

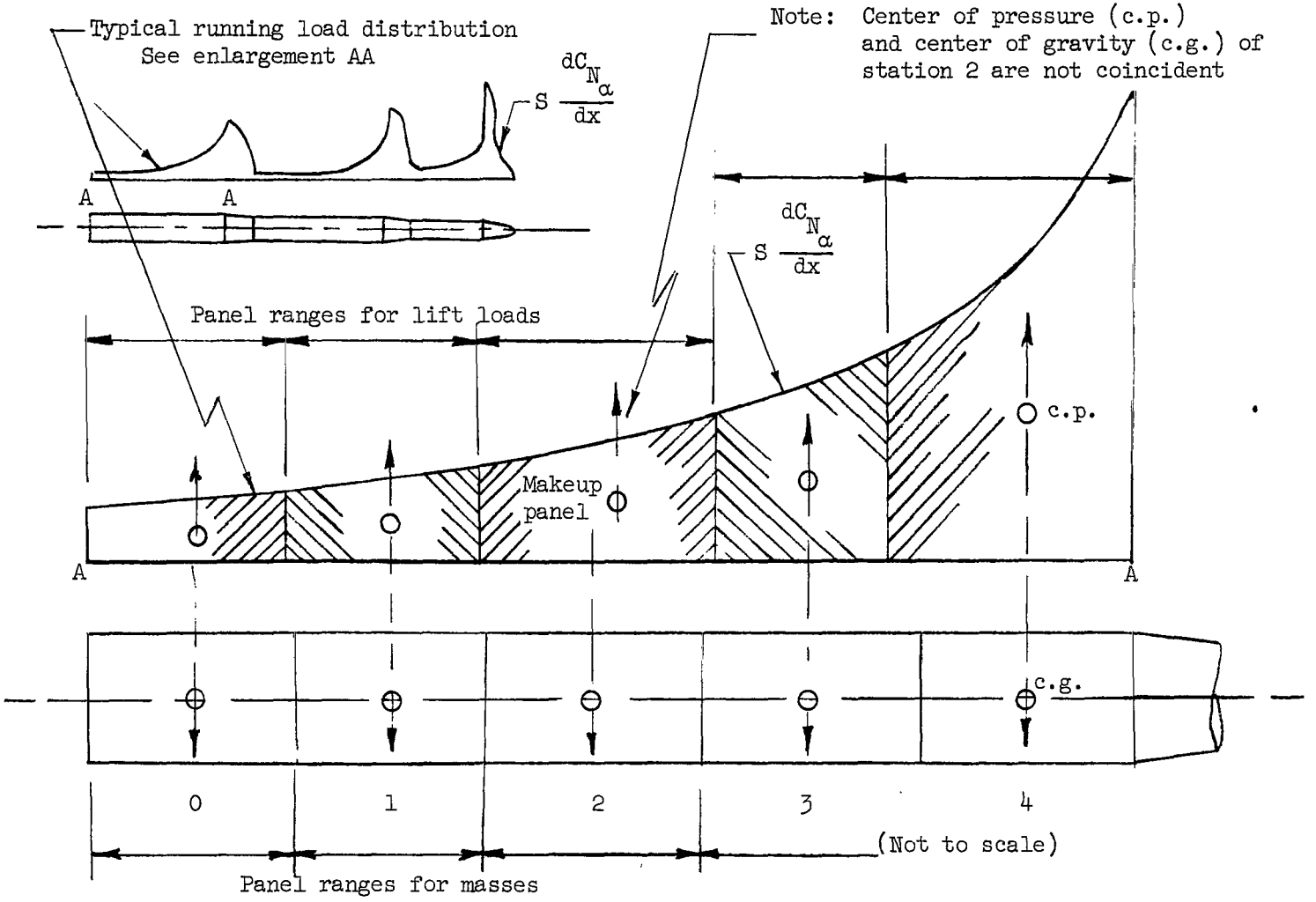

Figure 5.- Relationships between centers of pressure of discrete normal forces and centers of gravity of discrete masses.

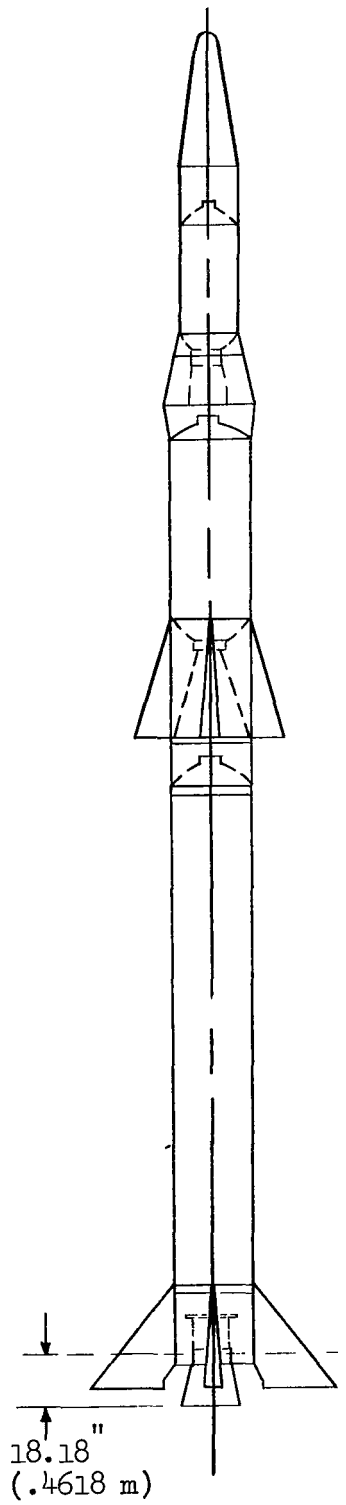

Station r	$\frac{x_r}{L}$	$\frac{m_r}{M}$	$\frac{C_{N_\alpha} S_r}{\overline{C_{N_\alpha} S}}$
22	.9356	.0032	.0250
21	.8902	.0105	.0610
20	.8478	.0291	.0234
19	.8124	.0440	.0158
18	.7822	.0440	.0085
17	.7509	.0466	.0072
16	.7267	.0035	.0204
15	.7004	.0108	.0511
14	.6762	.0409	.0130
13	.6459	.0985	.0357
12	.6056	.0985	.0234
11	.5652	.0985	.0229
10	.5288	.0326	.0123
9	.4945	.0087	.0144
8	.4570	.0275	.2612
7	.4037	.0537	.0174
6	.3482	.0630	.0093
5	.2977	.0313	.0092
4	.2473	.0310	.0063
3	.1918	.0370	.0084
2	.1312	.0367	.0059
1	.0706	.0362	.0096
0	0.0	.1140	.3385

L = 495.4 in. (12.58 m)

M = 16.938 lbf-sec^2/in. (2966.2 N-sec^2/m)

$\overline{C_{N_\alpha} S}$ = 7310.56 in^2/rad (4.716 m^2/rad)

Figure 6.- Vehicle geometry and analogous discrete system for RAM III vehicle at Mach 4.

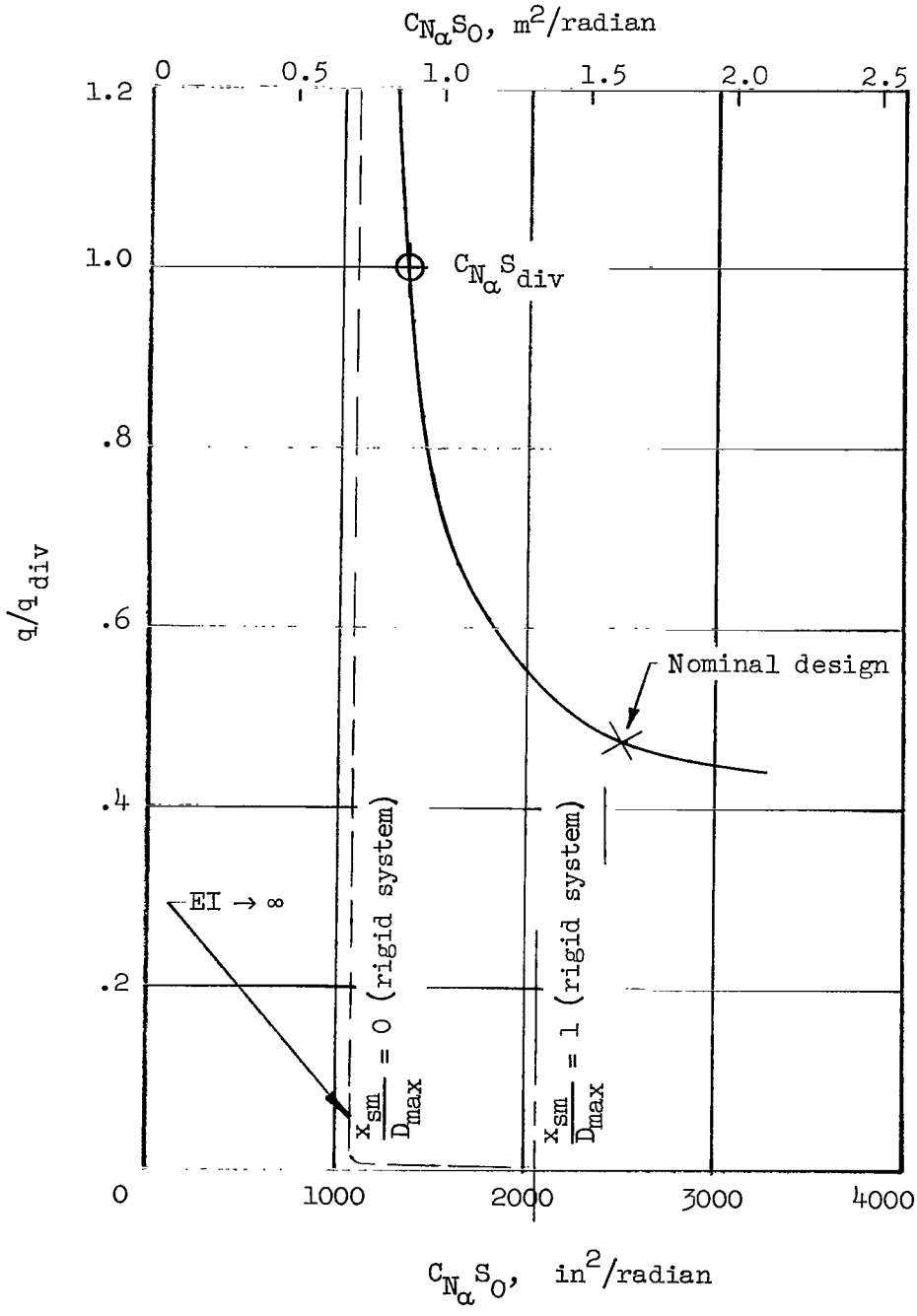

Figure 7.- Variation of q/q_{div} with zeroth panel normal-force coefficient for RAM III vehicle at Mach 4.

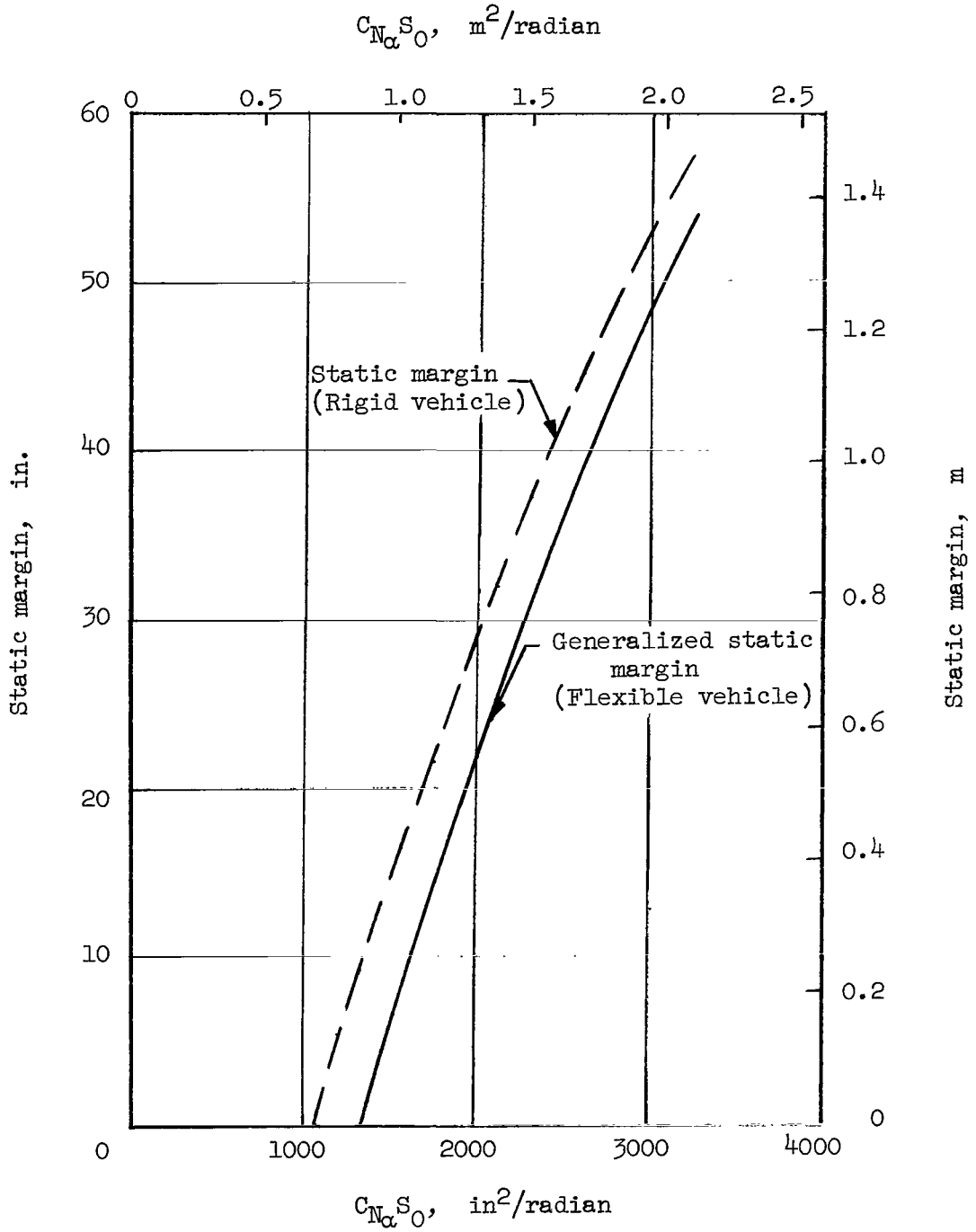

Figure 8.- Variations in generalized static margin and rigid-body static margin with $C_{N_\alpha}S_0$. RAM III vehicle; Mach 4.

VEHICLE LEGEND

1	○ Scout (unguided)	5	▽ SV-144	9	◁ 901
2	□ ARCAS TI-1673	6	◁ Scanner D71-3071	10	▽ 904
3	△ RAM III F65-3172	7	◇ SOCS SV63-3154	11	◇ Vector
4	◇ Pacemaker E69-3451	8	◇ Supersonic Decelerator E72-3746	12	▷ Aerobee 150

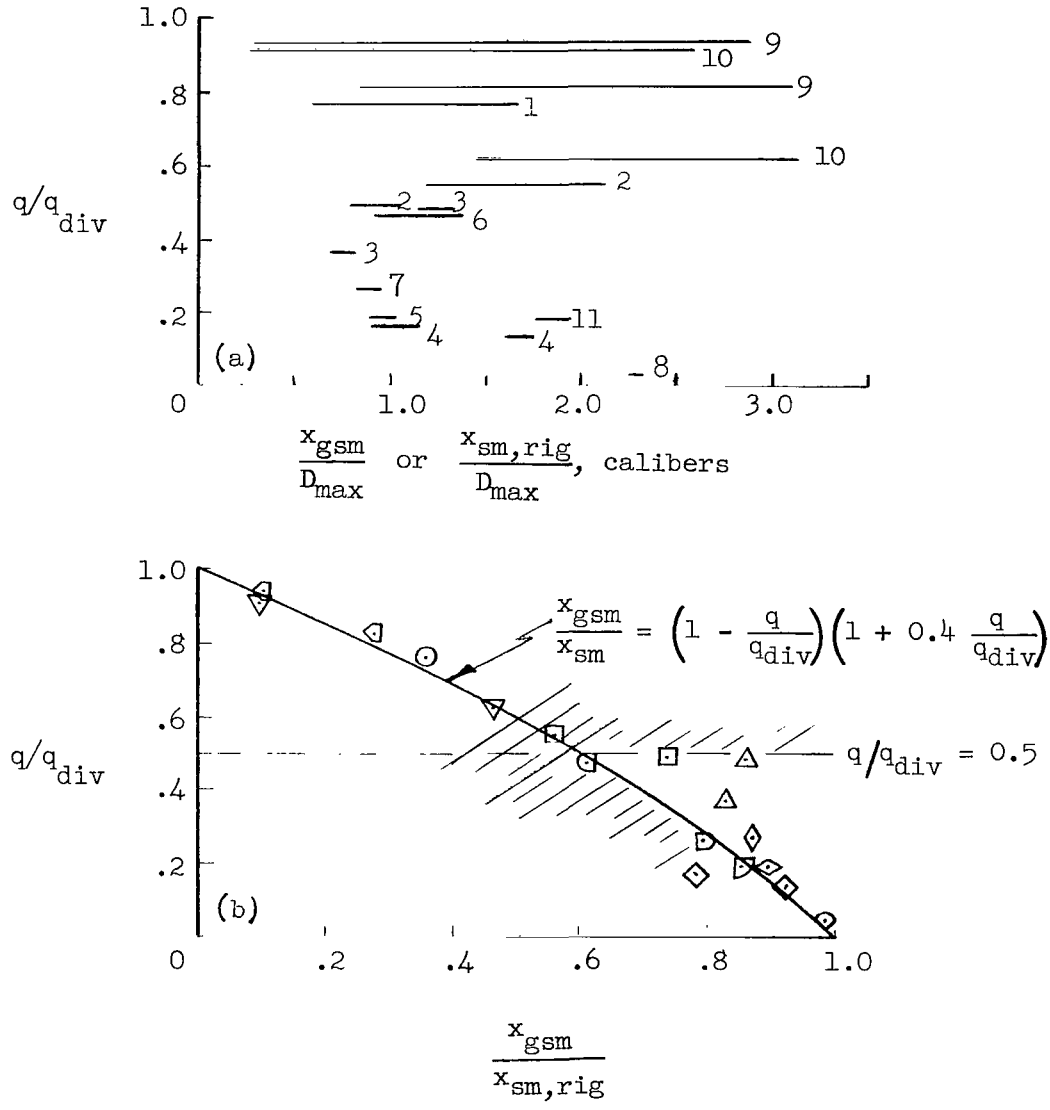

Figure 9.- Correlation between divergence dynamic-pressure ratio and generalized static margin.

"The aeronautical and space activities of the United States shall be conducted so as to contribute . . . to the expansion of human knowledge of phenomena in the atmosphere and space. The Administration shall provide for the widest practicable and appropriate dissemination of information concerning its activities and the results thereof."

—NATIONAL AERONAUTICS AND SPACE ACT OF 1958

NASA SCIENTIFIC AND TECHNICAL PUBLICATIONS

TECHNICAL REPORTS: Scientific and technical information considered important, complete, and a lasting contribution to existing knowledge.

TECHNICAL NOTES: Information less broad in scope but nevertheless of importance as a contribution to existing knowledge.

TECHNICAL MEMORANDUMS: Information receiving limited distribution because of preliminary data, security classification, or other reasons.

CONTRACTOR REPORTS: Technical information generated in connection with a NASA contract or grant and released under NASA auspices.

TECHNICAL TRANSLATIONS: Information published in a foreign language considered to merit NASA distribution in English.

TECHNICAL REPRINTS: Information derived from NASA activities and initially published in the form of journal articles.

SPECIAL PUBLICATIONS: Information derived from or of value to NASA activities but not necessarily reporting the results of individual NASA-programmed scientific efforts. Publications include conference proceedings, monographs, data compilations, handbooks, sourcebooks, and special bibliographies.

Details on the availability of these publications may be obtained from:

SCIENTIFIC AND TECHNICAL INFORMATION DIVISION

NATIONAL AERONAUTICS AND SPACE ADMINISTRATION

Washington, D.C. 20546